Tree Genetics & Genomes (2015) 11: 66
DOI 10.1007/s11295-015-0895-5

ORIGINAL PAPER

Overexpression of *CYCD1;2* in activation-tagged *Populus tremula* x *Populus alba* results in decreased cell size and altered leaf morphology

Martin Williams[1] · **Lisa Lowndes**[2] · **Sharon Regan**[2] · **Tannis Beardmore**[1]

Received: 11 March 2015 / Revised: 12 May 2015 / Accepted: 27 May 2015 / Published online: 6 June 2015

Abstract This paper includes the characterization of an activation-tagged mutant named *rippled leaf* that displays distinctive rippled-leaf morphology. Gene expression and microscopic analysis were done to characterize the *rippled leaf* mutant, and transgenic overexpression lines were generated and characterized using these methods. The *rippled leaf* mutant was found to have an activated *CYCLIN D1* (*CYCD1*;*2*), and overexpression of the gene using the 35S CaMV promoter resulted in plants with a highly similar leaf morphology. Microscopic analysis of the midvein of the *rippled leaf* mutant revealed that the mutant possessed significantly smaller and more numerous cortical parenchyma cells in its midvein compared with wild type. As well, in *rippled leaf*, the vascular tissue represented a larger proportion of the midvein. In transgenic lines, there was a similar change in cortical cell size, and an even larger proportion of the midvein was vascular tissue. In conclusion, a mutant with a leaf alteration phenotype was characterized. The *CYCD1*;*2* gene was found to be responsible for this phenotype, and the phenotype was recapitulated using overexpression of transgenic lines. Further studies with mutants such as *rippled leaf* are necessary for a better understanding of cell division and its relationship to plant growth and development.

Communicated by A. Brunner

This article is part of the Topical Collection on *Gene Expression*

✉ Martin Williams
Martin.Williams@NRCan.gc.ca

[1] Natural Resources Canada, Canadian Forest Service – Atlantic Forestry Centre, P.O. Box 4000, Fredericton, NB E3B 5P7, Canada

[2] Department of Biology, Queens University, Kingston, ON K7L 3N6, Canada

Keywords Activation tagging · Cell cycle · Cortical cell · Cyclins · Leaf morphology · Vascular tissue

Introduction

Growth and development in plants require cell division, cell elongation, and differentiation. Cell division (mitosis) is a systematic progression through a series of phases, terminating with chromosome duplication and chromosome segregation into daughter cells after mitosis (Smolarkiewicz and Dhonukshe 2013). For plants in the post-embryonic stage, cell division is restricted to meristems (root and shoot apical meristems, vascular and cork cambiums) and throughout developing leaf blades (reviewed in Gonzalez et al. 2012). In aerial plant structures, primary growth (leaves, stems, and flowers) is generated by the shoot apical meristem (SAM), whereas secondary growth is the result of the two lateral meristems, the vascular and cork cambiums (reviewed in Groover and Robischon 2006). Leaf morphogenesis is a developmental stage, where much work has focused on the role of cell cycling (Donnelly et al. 1999).

Leaf development, although not well studied in poplar (*Populus* spp.), has been extensively examined in *Arabidopsis*, where cell division occurs first in the leaf primordium initiated in the SAM. The dividing cells transition to the proliferation phase, where cell division and cell expansion are tightly regulated (Tsukaya 2014). Cells, first at the distal end of the developing leaf, stop mitosis and expand, and a resultant gradient of expanding cells occurs from the proximodistal axis, whereas growth from areas of the lateral meristem originates from the central dorsal area. The lamina continues growth by cell expansion; additionally, cell differentiation occurs within tissue layers as distinct planes of orientation are laid down. Evidence suggests that there are

temporally two stages of arrest/cessation in leaf development: the first is a cessation of growth in the abaxial and adaxial epidermis, the palisade and spongy parenchyma cells; the second stage occurs later and is associated with the arrest of meristemoids (transitional state in the cell lineage producing stomata) and procambial cells (proto-xylem and proto-phloem). The final shape of the cells and hence the leaf occurs after complete cell expansion.

There are five phases of the cell cycle (Gap 0 (G0), Gap 1 (G1), Synthesis (S), Gap 2 (G2), and Mitosis (M)), with two major control points, the transitions from G1-to-S and G2-to-M (Van't Hof 1966). During the S-phase, nuclear DNA is replicated, so the control of the G1-to-S-phase transition is a key regulatory step because cells typically become committed to divide after they have replicated their DNA (De Veylder et al. 2007). The M-phase results in the separation of sister chromatids into the newly forming daughter cells. Among the main cell cycle regulators controlling these phase transitions is a specific class of serine-threonine protein kinases, cyclin-dependent kinases (CDKs), and cyclins, essential regulators of CDKs (Arias et al. 2006). Cyclins activate CDKs by complexing with the CDK catalytic unit, changing the conformation of their catalytic sites (Gutierrez 2009). The CDKs then phosphorylate numerous substrates (i.e., retinoblastoma-related protein (RBR)) at the cell cycle transition points, triggering DNA replication and mitosis. Additionally, cyclins contribute to the selection of CDK substrates and are involved in subcellular localization and the regulation of protein stability (Menges et al. 2007).

In plants, cyclin-like proteins can be divided into different types based on phylogenetic analysis and sequence similarity (reviewed by Wang et al. 2004; Gutierrez 2005). Among these, A-, B-, and D-type cyclins have been the most extensively studied because they are conserved in many different plants and animals and have proven to be highly important to the cell (Renaudin et al. 1996). There are specialized functions associated with the different types of cyclins. For example, A- and B-type cyclins and corresponding CDKs are associated with the G2-M transition (Magyar et al. 1997; Ito et al. 1998), whereas D-type cyclins are typically associated with G1 stage and G1-to-S transition (Oakenfull et al. 2002; Guo et al. 2005) but also in the G2-M transition (De Veylder et al. 2007). In the *Populus trichocarpa* genome, 22 CYCD genes have been found (Tuskan et al. 2006), and 5 of the 22 genes are members of the CYCD1 subgroup.

Similar to other cyclins, D-type cyclins bind to the CDK catalytic subunit; CYCD–CDK complexes phosphorylate RBR, which results in the dissociation of the RBR from promoter-bound E2F/DP complexes (Uemukai et al. 2005). This then triggers the expression of specific genes involved in DNA replication and allows the cell cycle to progress into the S-phase (Uemukai et al. 2005; Menges et al. 2007). In poplar, no information, apart from gene sequence data (Menges et al. 2007), is available concerning cyclin Ds. Among the *CYCD1* subgroup, two genes (*CYCD1*;*1* and *CYCD1*;*2*) are orthologs that are almost identical (Menges et al. 2007) at the sequence level. However, cyclin Ds have been found to be expressed in early developmental events in other plant species. For example, in *Cucumis sativus*, *CYCD3*;*1*, *CYCD3*;*2*, and *CYCD3*;*3* expression is correlated with cell cycle events in fruit development (Cui et al. 2014), whereas during *Zea maize* seed germination and early seedling growth (i.e., mesocotyl, root tips, and first leaf), *CYCD4*;*2*, *CYCD5*;*3a*, and *CYCD5*;*3b* were expressed and exhibited temporal variation in each of their expression patterns (Buendía-Monreal et al. 2011). Gaudin et al. (2000) found evidence that cyclin D expression can be specific to cell populations with different fates, and there may be a link between the regulation of the cell division cycle and the pattern of plant development. They examined the expression of three cyclin D genes (*CYCD1*, *CYCD3a*, *CYCD3b*) in *Antirrhinum majus* meristems and they observed unique spatial and temporal expression of *CYCD1*, *CYCD3a*, and *CYCD3b* during all cell cycle phases. The *CYDCD1*, *CYDCD3b* were expressed throughout the apical meristems, and *CYDCD3a* expression was restricted to the peripheral region of the meristem; however, in the floral meristems, *CYCD3b* expression increased in the boundary zones between primordia, during petal morphogenesis, and also in the anther. In assessing the impact of cyclin Ds on growth, it has been observed in *Arabidopsis* that overexpression of *CYCD1* causes an increase in the overall size of the plant (Cho et al. 2004), whereas the induction of *CYCD1* from *A. majus* in cultured tobacco cells speeded up the entry of the G0 and G1 phases into S-phase, as well as hastened the progression through both the S and G2 phases, leading to an increase in cell growth rate (Koroleva et al. 2004). These results suggest that cyclin Ds may have a role in regulating cell division and plant development and in determining growth rate.

The objective of this work was to characterize the poplar activation-tagged line called *rippled leaf* (Harrison et al. 2007), which displays altered leaf morphology that appears to originate from an undulating midvein. It was found that overexpression of the gene *CYCD1*;2, a key regulator of cell cycle progression, is responsible for this phenotype, an undulating lamina, midrib, and petiole morphology. This is the first mutant of *CYCD1*;*2* that has been described in plants and will help to differentiate the unique roles of D-type cyclins in plant development. Understanding the molecular networks involved in cell cycling would be highly beneficial for understanding the processes involved in plant growth, in particular those associated with biomass production. Among these highly controlled processes, cell division and expansion are important in terms of impacts on growth because accelerating these processes could potentially increase growth rates.

Material and methods

Plant material

Trees were grown in a greenhouse under natural daylight and temperature conditions at the Canadian Forest Service (CFS), Fredericton, New Brunswick, Canada, or under controlled greenhouse conditions (22–26 °C at Queen's University, Kingston, Ontario, Canada). The *rippled leaf* mutant was generated as described by Harrison et al. (2007) in the *Populus tremula* × *Populus alba* INRA 717-1-B4 background, and all comparisons of *rippled leaf* were made to the hybrid (WT). The *rippled leaf* mutant was identified during the initial phenotypic screening of the mutants based on the leaf phenotype.

Phenotypic analysis of the mutant

Cuttings of WT and *rippled leaf* were established by cutting 4- to 5-cm shoot explants from 2- to 3-year-old stock plants and growing them in natural greenhouse conditions for 9 weeks. Four trees each of WT and *rippled leaf* were randomly selected, and height, number of leaves, and stem diameter were measured. To assess biomass, cuttings of WT and *rippled leaf* were established as described above and, after 2 months of growth, were transplanted into 15 cm diameter pots. Following 3.5 months of growth, a triplicate of each line was randomly selected, and the leaves, stems, and roots were harvested, weighed, and dried separately for 72 h at 50 °C before weighing again after complete dehydration. A Student's *t* test was performed to determine the significance of the results for comparison of *rippled leaf* and WT physiological parameters ($P<0.05$).

Identification of the gene responsible for the *rippled leaf* phenotype

Southern blot analysis of the *rippled leaf* mutant had previously revealed the presence of a single T-DNA insertion event (Harrison et al. 2007). The location of the insert was determined using Genome Walker™ universal kit (Clontech, http://www.clontech.com), according to the manufacturer's instructions. Total RNA was extracted from all tissues using a modification of Chang et al. (1993; CTAB followed by QIAGEN RNeasy kit). Total RNA was quantified using the nanodrop 1000 spectrophotometer and DNaseI-treated prior to RT-qPCR. The expression levels of three genes: unknown (Potri.008G146500); *CYCD1*;*2* (Potri.008G146600); unknown (Potri.008G146700), within 20 kb either upstream or downstream from the insertion site were tested in the leaves using the one-step Quantitect SYBR Green RT-qPCR kit (QIAGEN, http://www.qiagen.com) according to manufacturer's instructions, using a DNA Engine Opticon™2 real-time PCR system (Bio-Rad, http://www.bio-rad.com). In addition to these three genes, two more genes of interest: *RBR* (Potri.001G031400) and *CDKA* (Potri.004G133500) involved in cell cycle progression, were assessed using the same procedure as stated above. Primers used for the analyses were as follows: *CYCD1*;*2* forward, 5′-AGCTCGATCCAGCAGGAGCCTATACTGG-3′, *CYCD1*;*2* reverse, 5′-CGCAGCAATGCTAGATGGCCTATACTCAA-3′, *14590* forward, 5′-AAGTTATGAAGGTGATACGGGC-3′, *14590* reverse, 5′-TGACCTTAGTGAAGCAGAGTTG-3′, *14610* forward, 5′-AAGTTATGAAGGTGATACGGGC-3′, *14610* reverse, 5′-ACATGCACACGAATGCCAGTTG G-3′, *RBR* forward, 5′-GCCAGCAATATCCAATGAAGC-3′, *RBR* reverse, 5′-ACAGCCAGTACAGAAACCAG-3′, *CDKA* forward, 5′-ACGAGGGCGTACCCAGCACTG-3′, *CDKA* reverse, 5′-GGCAGTAAGCAATGCCACGGAGA-3′, *GAPDH* forward, 5′-AGCTCGATCCAGCAGGAGCC TATACTGG-3′, *GAPDH* reverse, 5′-CGCAGCAATGCTAG ATGGCCTATACTCAA-3′. To compare endogenous levels of genes of interest between different tissues of WT, mean normalized expression (MNE) were calculated using Q-Gene (Perikles 2003). Fold difference ratios between *rippled leaf* and WT were also calculated using Q-Gene. Both fold difference ratios and MNE were calculated using *GAPDH* (Potri.010G055400) as the reference gene for normalization. The *GAPDH* gene used as a reference was tested under experimental conditions and found to be stably expressed. Leaf samples were taken according to Hartmann et al. (2000), where leaf development was divided into four different stages, which characterized them from shoot apex to stem (above soil) as (1) developing, (2) expanding, (3) mature, and (4) old mature. One of the samples was taken from the bottom third closer to the base of the stem (mature/old mature leaves), another from the top closer to the shoot apex (developing/expanding leaves), and the last from the middle, which would include expanding/mature leaves, but this leaf sample was from second-year wood. All experiments were performed on three biological replicates, where each sample was measured in two technical replicates.

The *PtaCYCD1*;*2* cDNA was isolated using the Smart RACE kit (Clontech, http://www.clontech.com) according to manufacturer's instructions. The *PtaCYCD1*;*2* cDNA CDS was subcloned in pART7 and subsequently in pART27 (Gleave 1992) and transformed into WT 717-1-B4 poplar as described by Harrison et al. (2007). Out of 11 independent transgenic lines recovered (*PtaCYCD1*;*2*), 6 lines (oe6-oe11) were analyzed for *CYCD1*;*2* gene expression. Each line was analyzed in duplicate technical replicates.

Microscopic analysis of the mutant

Leaf and stem samples were taken from both WT and *rippled leaf* trees. The stage of the leaves was determined according to the Plastochron index (Erickson and Michelini 1957; Larson

and Isebrands 1971); only leaves of the same index were directly compared. Midveins were sectioned in the middle of the leaf by hand using a razor blade and stained for 1 min with 0.01 % Toluidine Blue O in 1 % boric acid. Tissues were observed under a Zeiss Axio Imager Z1 light microscope; photographs were taken using an integrated Zeiss AxioCam HRc. Both longitudinal- and transverse-sectioned midvein images were analyzed using the AxioVision Release 4.6 computer program to determine the proportion of vascular vs. cortical tissue in each section and to measure the size of cells in the midvein. For the vascular vs. cortical tissue comparison, 15 WT leaves, 15 *rippled leaf* leaves, and 5 leaves from transgenic lines 10 were compared.

Results

The *rippled leaf* mutant has altered leaves and petioles

A screen of 1800 activation-tagged poplar lines revealed line E19–12, named *rippled leaf*, which exhibits unusual leaf morphology. Although the *rippled leaf* tree appears similar to the WT in terms of stature and branching (Fig. 1a), the leaves have a distinctive rippled phenotype that is found in the midvein and the lamina (Fig. 1a inset). The midvein undulates, and this alteration is also seen in the petioles, which have more curvature than the WT petiole (Fig. 1a–c). This altered leaf and petiole morphology was found to be very stable in this mutant, even under long-term field conditions (5-year-old field-grown trees, Fig. 1b). When the leaves are compared according to their plastochron index (Fig. 1c), the leaves of the mutant begin to diverge from WT at plastochron 1 and display the full phenotype by plastochron 3. In later stages of leaf development (plastochron 7–13; Fig. 1c), the extreme *rippled leaf* phenotype is replaced by a more subtle undulating midvein with less distinct undulating of the lamina. From plastochron 5 and onward, the tips of the leaves are often curled downward. In addition to the changes in leaf morphology, the leaves of *rippled leaf* are smaller. To assess any impact on tree growth, we compared the height, stem diameter, leaf number, and dry weight biomass of young *rippled leaf* and WT (3.5 months old) plants (Table 1). No

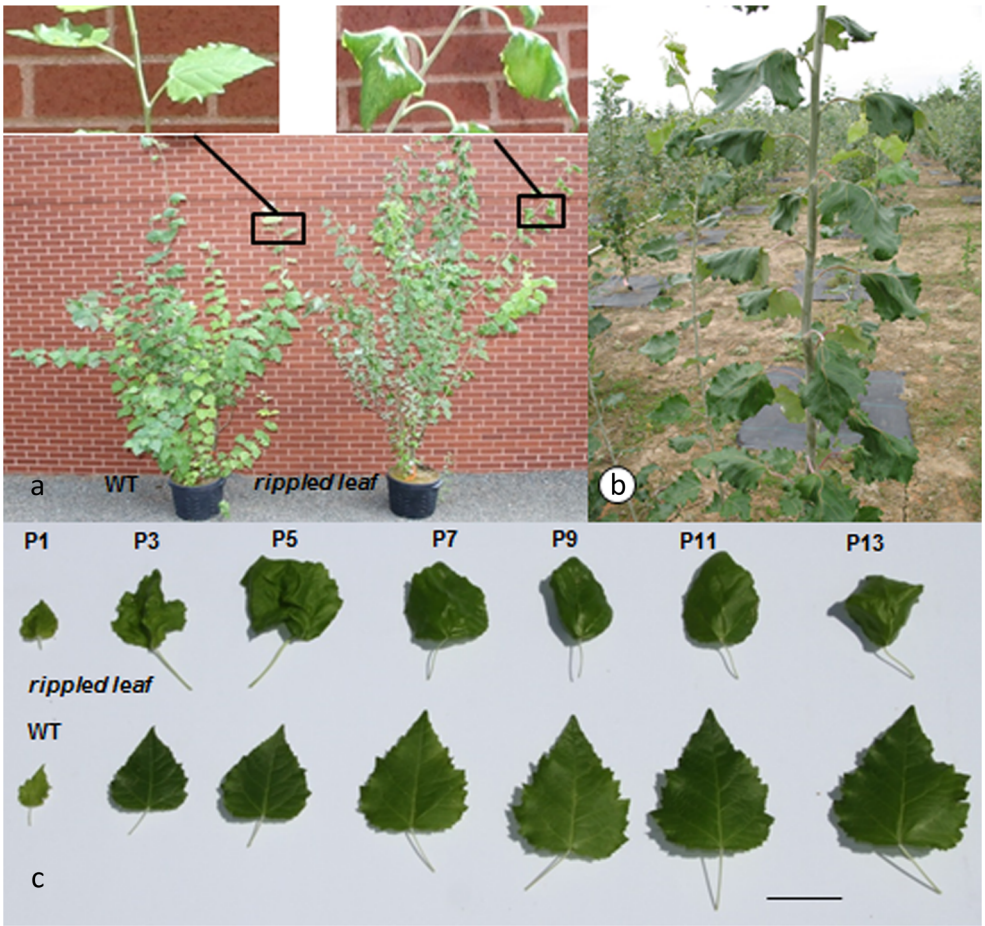

Fig. 1 Comparison of WT and *rippled leaf* mutant **a** Greenhouse-grown 5-year-old WT (*left*) and *rippled leaf* mutant (*right*). **b** Field-grown 5-year-old *rippled leaf* tree showing the rippled leaf morphology in the mutant. **c** WT and *rippled leaf* leaves from Plastochron index P1 to P13 showing the rippled leaves and curved petiole phenotype. *Scale bar* 5 cm. Photograph **b** is courtesy of Dr. Steven Strauss and is from his field trial of the activation-tagged lines in Corvallis, Oregon

Table 1 Comparison of plant size and biomass for *rippled leaf* and WT Morphological characteristics of wildtype (WT) and *rippled leaf* poplar plants

	WT	*rippled leaf*
Height (cm)	42.1±3.1	47.6±3.0
Stem diameter (base) (mm)	3.28±0.18	3.80±0.25
Stem diameter (middle) (mm)	2.23±0.05	2.54±0.13
Stem diameter (apex) (mm)*	0.96±0.04	1.08±0.03
Root biomass (g)	1.23±0.12	0.73±0.18
Stem biomass (g)*	1.39±0.10	0.97±0.10
Leaf biomass (g)*	1.95±0.08	1.37±0.14
Total plant biomass (g)*	4.58±0.29	3.07±0.42

Results presented are the measurements from three WT and *rippled leaf* greenhouse-grown plants±SE. Measurements were made on 3.5-month-old plants. Stem diameters were measured in three locations: the base of the plant, half the stem height (middle), and immediately below the apical meristem (referred to as the apex). Biomass measurements are on a dry weight basis. Asterisk indicates statistical significance based on Student's *t* test ($P<0.05$)

significant differences were found between plant height and stem diameter, but leaf and stem biomass was significantly lower in *rippled leaf* compared with WT. The decrease in *rippled leaf* biomass was 43 and 42 % for the stems and leaves, respectively, compared with WT biomass (Table 1). Timing of bud set and bud break assessed over two growing seasons in 3- to 4-year-old plants was the same (results not shown).

CYCD1;2 is upregulated in *rippled leaf*

As reported previously (Harrison et al. 2007), only one T-DNA insertion was present in the *rippled leaf* mutant as measured by Southern blot analysis. The T-DNA insertion site was found to be located on chromosome 8 at position 9870557 (Fig. 2a). Two predicted gene models were found downstream of the 35S tetramer enhancers, Potri.008G146600 (encoding a putative cyclin D1 (*CYCD1;2*)), at −5.6 kb and Potri.008G146700 (encoding a gene with unknown function) at −16 kb, and one upstream gene model Potri.008G146500 (encoding a gene with unknown function) was found at +15 kb. The transcript abundance of the three genes was determined by reverse transcriptase-quantitative PCR (RT-qPCR), and only the putative cyclin D1, *CYCD1;2* was found to be overexpressed in *rippled leaf* (Fig. 2b). Transcript abundance of *CYCD1;2* in various tissues revealed a 3- to 24-fold increase in expression, with the highest in the leaves, which is consistent with the prevalent mutant leaf phenotype (Fig. 3a). To assess whether the increase in *CYCD1;2* expression has an impact on the expression of other cell cycle genes, we compared *CDKA* (Fig. 3b) and *RBR* (Fig. 3c) transcript levels between *rippled leaf* and WT, and there were no significant differences in the tissues tested. Endogenous levels of *CYCD1;2 CDKA* and *RBR* were evaluated in multiple tissues, and results show that basal levels of *CYCD1;2* (Fig. 3d) are the highest in the

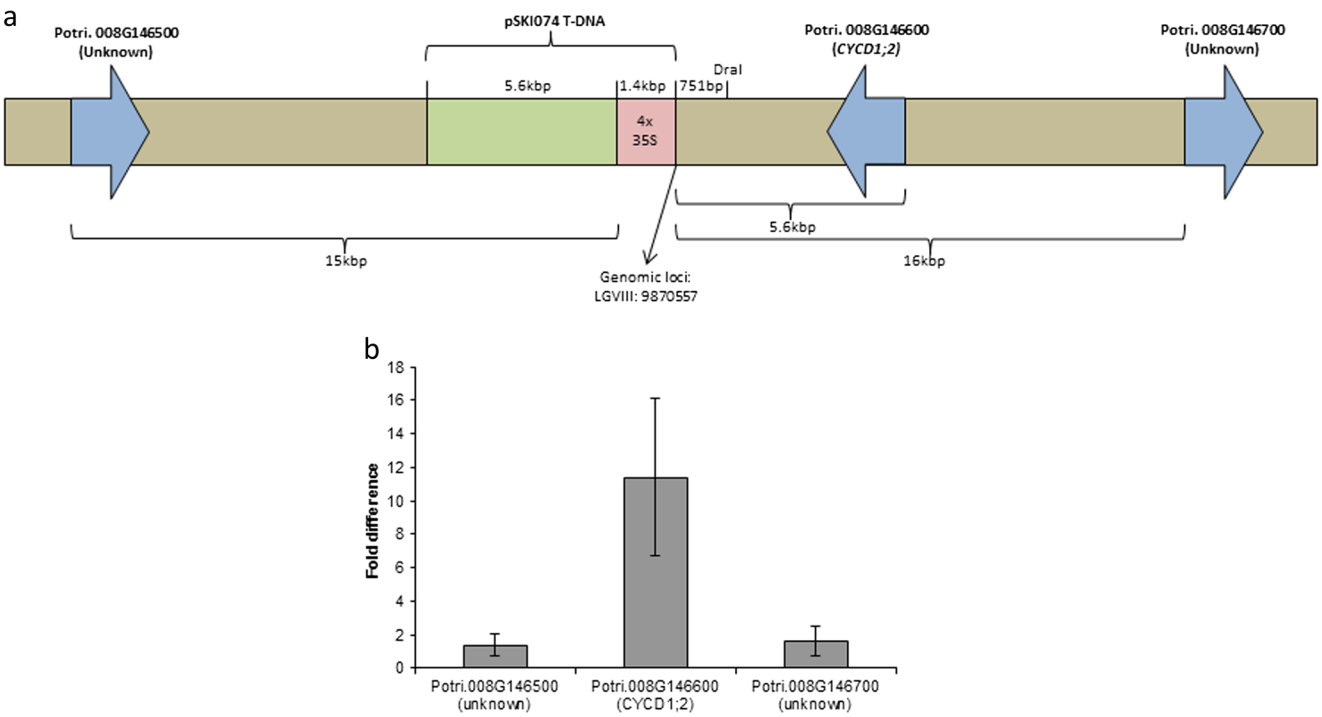

Fig. 2 **a** Representation of *rippled leaf* T-DNA insertion site on chromosome 8 showing the genes adjacent to the insertion site. **b** Gene expression analysis of genes adjacent to the *rippled leaf* T-DNA insertion site. Gene expression results are fold change differences between *rippled leaf* and WT. The data were normalized against the *GAPDH* reference gene. *Bars* represent mean±SE

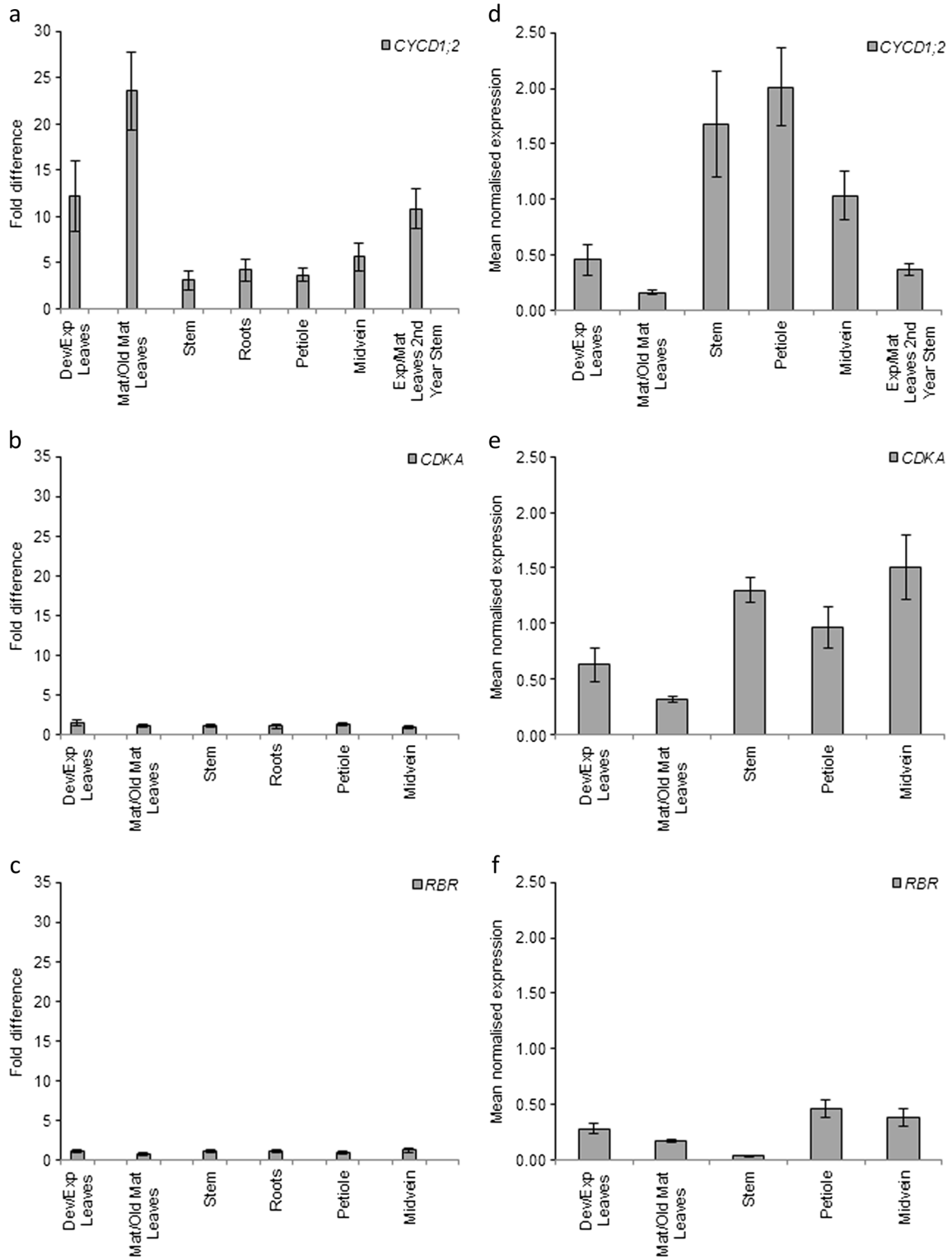

Fig. 3 Fold difference ratios for **a** *CYCD1;2*, **b** *CDKA*, and **c** *RBR* between WT and *rippled leaf* were measured in multiple different poplar tissues. Endogenous levels of **d** *CYCD1;2*, **e** *CDKA*, and **f** *RBR* were measured in multiple tissues of WT. Fold difference ratios and mean normalized expression (MNE) were calculated using Q-Gene software. Dev/Exp leaves = developing/expanding leaves; Mat/Old Mat leaves = mature/old mature leaves; Exp/Mat leaves = expanding/mature leaves. The data were normalized against the *GAPDH* reference gene. Bars represent mean±SE

stem petiole and midvein samples and lowest in the leaf samples. The same trend was observed for *CDKA* (Fig. 3e), while for *RBR* (Fig. 3f), transcript abundance is highest in the petiole and decreases in the developing

leaves, then in mature, older leaves and is the lowest in the stem. Expression levels for *CYCD1*;*2* and *CDKA* were higher than *RBR* for all tissues tested. Additionally, the relative proportion of *CYCD1*;*2* and *CDKA* were similar, but did not occur in *RBR*.

Cell size is altered in the midvein of the *rippled leaf* mutant

To determine one of the causes of the *rippled leaf* phenotype, we compared the anatomy of the *rippled leaf* midvein to that of WT (Fig. 4). Toluidine blue O staining of hand-cut sections of the WT midvein reveals the arrangement of tissues in a transverse section of a fully expanded leaf (Fig. 4a, b) and in a longitudinal section (Fig. 4c), where the epidermal cells (EC), cortical cells (CC), phloem fibers (PF), phloem (Ph), xylem (X), and inner pith (Pi) are easily distinguished. In the *rippled leaf* mutant, the arrangement of the tissues was the same as WT, but there is a higher proportion of vascular tissue compared with the WT (Fig. 4a, d). On average, the vasculature in the midvein of *rippled leaf* covers 35.4 % of the cross-sectional area, which is significantly greater than the 32.1 % seen in the WT (Table 2). These transverse sections did not reveal a consistent difference in the size of cells in any tissue of the midvein between WT and the *rippled leaf* mutant (compare Fig. 4a and b to d and e). In contrast, longitudinal sections of WT and *rippled leaf* midveins revealed differences in the length of cells, especially in the cortical tissue. Because they are easier to differentiate, the lengths of cells in the cortex

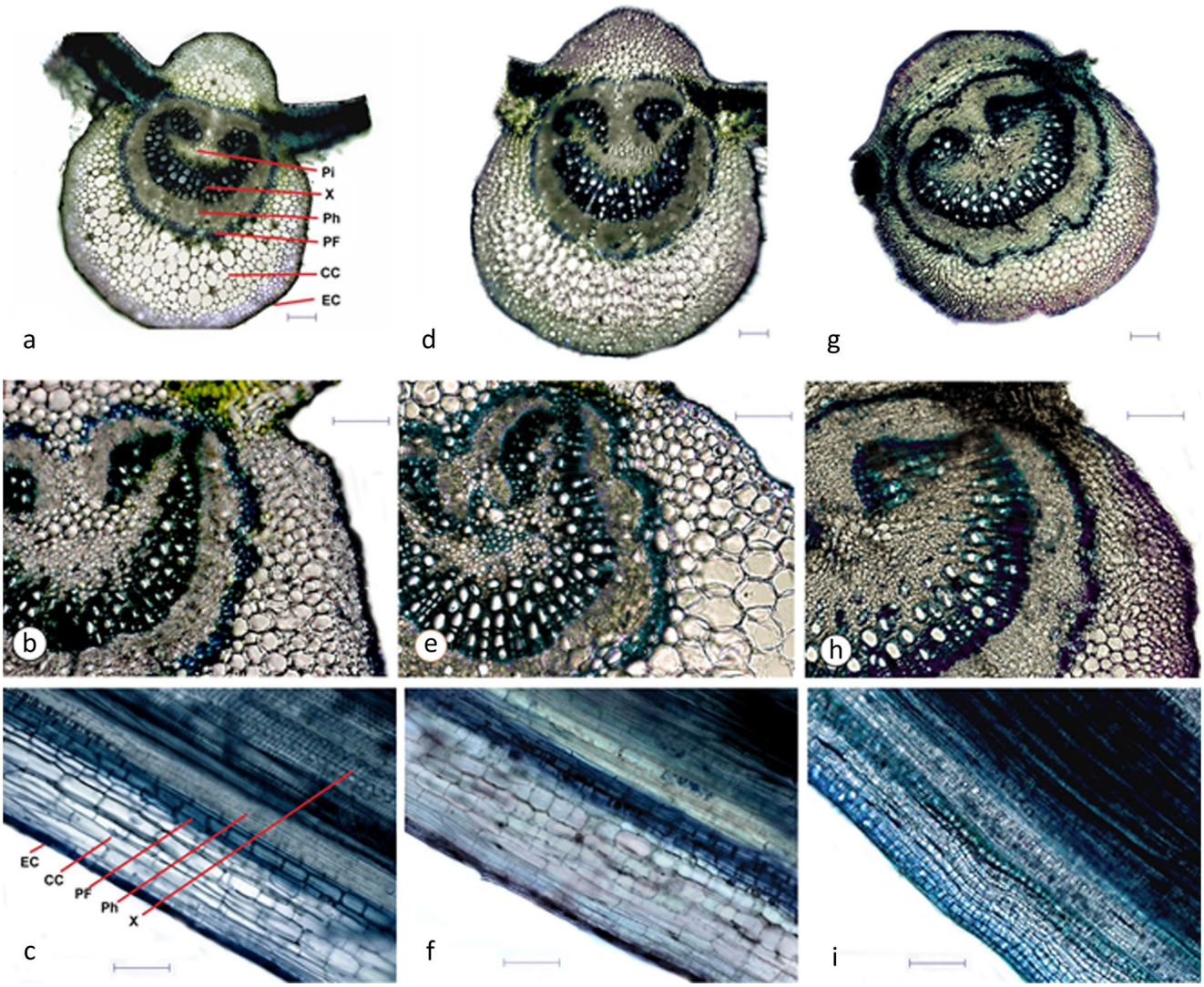

Fig. 4 Comparison of WT, *rippled leaf*, and *PtaCYCD1-2* oe line 10 midveins. Panels **a**, **b**, **d**, **e**, **g**, **h** are cross-sections, whereas **c**, **f**, **i** are longitudinal sections. Panels **a**–**c** are WT; note their long, regular cells and relatively small vascular bundle proportion. Panels **g**–**i** are the *PtaCYCD1-2* overexpression line 10; by comparison, its cells are small, numerous, and the proportional size of its vascular bundle is much larger. Panels **d**–**f** are *rippled leaf*; its characteristics are similar to those seen in the *PtaCYCD1*;*2* overexpression line 10 to a less extreme degree. Panels **a**, **d**, **g** are at ×100 magnification, whereas panels **b**, **c**, **e**, **f**, **h**, **i** are ×200 magnification. *Scale bars* all represent 100 μm

Table 2 Comparison of cortical longitudinal cell length and midrib vasculature ratio for WT, *rippled leaf*, and *PtaCYCD1;2* overexpression line 10

	WT	n	*rippled leaf*	n	*PtaCYCD1;2* oe line 10	*n*
Longitudinal cell length						
Innermost row	51.33±1.58	235	36.28*±0.73	317	21.11*±0.68	345
3rd row	86.16±3.16	136	46.43*±1.44	223	20.32*±0.84	321
6th row	54.11±1.23	224	43.03*±0.97	250	23.02*±0.94	333
Midrib vasculature ratio	0.321±0.003		0.353*±0.004		0.468*±0.006	

Results presented represent the mean measurements taken from WT, *rippled leaf*, and *PtaCYCD1y2* overexpression (oe) line 10 greenhouse-grown plants±SE. The midrib vasculature ratio is the proportion of the cross-section of the midrib that is taken up by the vasculature. Asterisk indicates statistical significance based on Student's *t* test ($P<0.05$)

were measured along three cell files, the third and sixth cell file from the epidermis as well as the innermost file next to phloem fibers. Comparison of all three cell files revealed that the *rippled leaf* cells were significantly shorter than WT (Fig. 4c, f and Table 2).

Overexpression of *PtaCYCD1;2* causes a *rippled leaf* phenotype

To verify that *PtaCYCD1;2* is responsible for the *rippled leaf* phenotype, the coding sequence was introduced into WT under the control of the 35S CaMV promoter. Eleven independent overexpression (oe) transgenic lines were created, and 6 (*PtaCYCD1;2* lines oe6-11) were chosen for further analysis. Four out of the six lines showed higher transcript abundance for *PtaCYCD1;2*, ranging from a 2.5- to a 81-fold difference, whereas the other two were similar to WT in leaves (Fig. 5). Line 10 exhibited the highest *PtaCYCD1;2* levels with a 81-fold increase over WT. Line 10 also displayed a rippled leaf phenotype that was very similar to the mutant (Fig. 6a, b). In these lines, the rippling was more pronounced, as was the downward curvature of the leaf tip (compare Fig. 1c and Fig. 6a, b). A transverse section of the leaf midvein from these overexpressing lines revealed a typical arrangement of the tissues, but the vascular tissue contributed to a higher proportion (46.8 %) of the midvein area than was found in WT (32.1 %) and *rippled leaf* (35.4 %) (see Table 2). A longitudinal section of the midvein of the overexpressing lines showed that the cells were significantly smaller than WT and *rippled leaf* (Fig. 4c, f, i). In these lines, the rippled phenotype was not restricted to the leaves, but resulted in a twisted phenotype in the stem (Fig. 6c). These results support the hypothesis that an increase in *CYCD1;2* expression is responsible for the rippled morphological phenotype seen in the *rippled leaf* mutant.

Discussion

Overexpression of the *PtaCYCD1;2* gene is responsible for the *rippled leaf* phenotype

The molecular networks that regulate the main processes involved in growth, such as cell division and expansion, have not been clearly elucidated. In screening a population of activation-tagged lines, a poplar mutant with rippled leaves and midvein was identified (Harrison et al. 2007). Characterization of the *rippled leaf* insertion site along with gene expression measurements of genes within 20 kb of the insert showed that only *PtaCYCD1;2* was overexpressed. To confirm that *PtaCYCD1;2* is responsible for the altered phenotype in this mutant, several transgenic lines with the *PtaCYCD1;2* gene under the control of the 35S promoter were created, and in two of these lines, a phenotype similar to *rippled leaf* was found. The leaf alteration phenotype in the *PtaCYCD1;2* oe line 10 was more pronounced than in the original *rippled leaf*

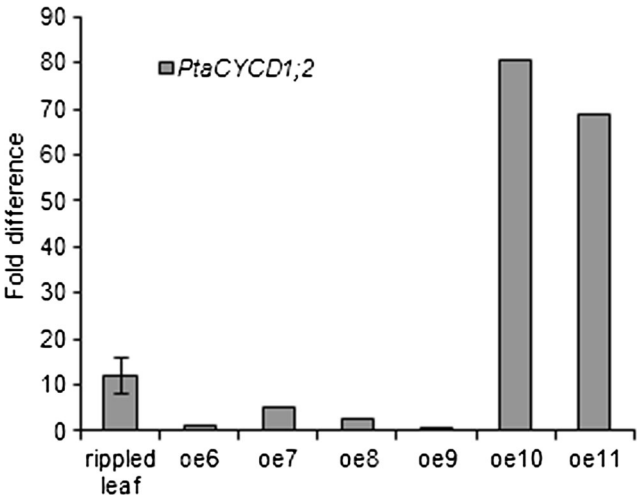

Fig. 5 Gene expression analysis of *CYCD1;2* from poplar leaf tissue in multiple *rippled leaf PtaCYCD1-2* overexpression lines (oe). Gene expression results are fold change differences between *rippled leaf* or *PtaCYCD1;2* transgenic lines and WT. The data were normalized against the *GAPDH* reference gene. *Bar* represent mean±SE

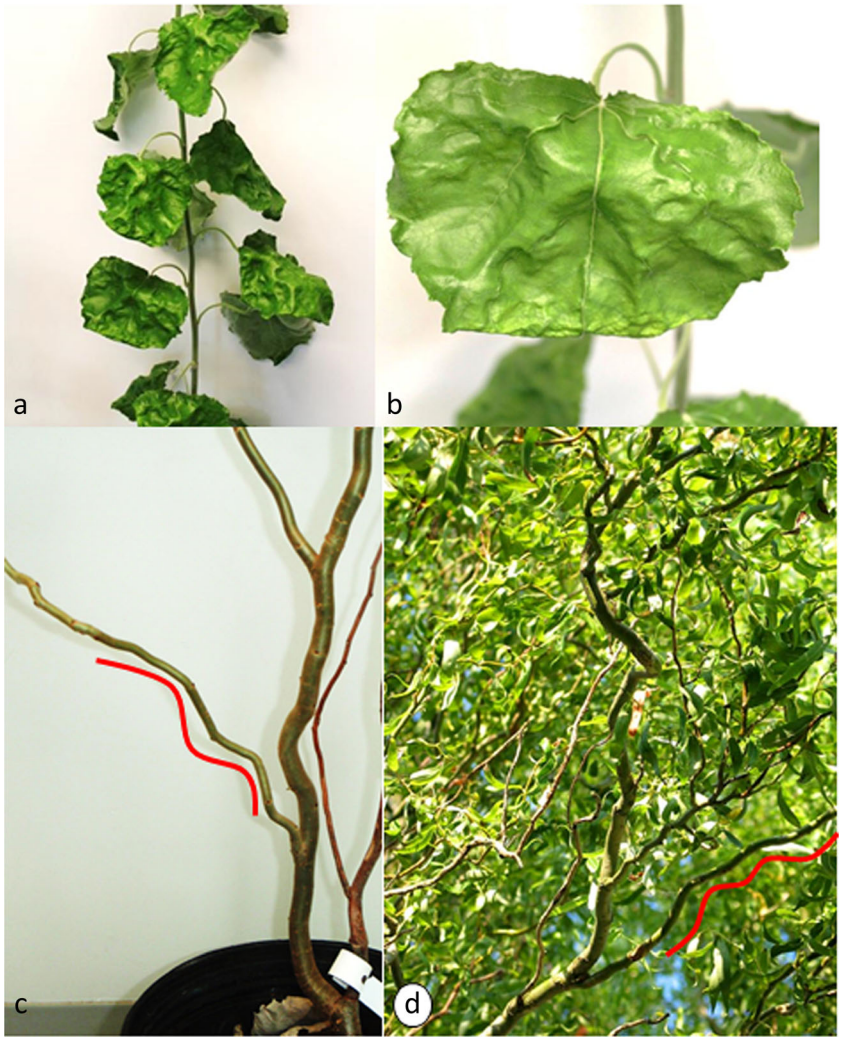

Fig. 6 Pictures of **a** transgenic line overexpressing *PtaCYCD1*;*2* and **b** close-up of a leaf. The stem of a *PtaCYCD1*;*2* overexpression line displays a distinct wavy phenotype **c** that is reminiscent of the stem of the **d** Corkscrew willow (*Salix matsudana*, Koidz. Cultivar 'Tortuosa'The *red lines* in **c**, **d** highlight the similarity in stem structure. Photograph **d** is courtesy of Hans-Cees Speel (bomengids.nl)

activation-tagged line, where the cells were even smaller and the proportion of the vascular tissue was even larger than in *rippled leaf*. The transcript abundance of *CYCD1*;*2* was also significantly higher in *PtaCYCD1*;*2* oe line 10 than in *rippled leaf*. The more enhanced phenotype in these overexpressing transgenic lines is potentially due to the overexpression itself or to the ectopic expression by the 35S promoter in many different cells rather than the enhanced native expression enhanced by the 35S enhancer in the correct cell types of *rippled leaf* or both. Since endogenous levels of *CYCD1*;*2* varies within different tissues in WT and that oe lines are driven by a constitutive 35S promoter, it is highly probable that the extreme phenotype observed in oe L10 is a result of both processes.

Although numerous plant studies have assessed the overexpression of genes from the cyclin D subgroup, only a few studies (Cho et al. 2004; Koroleva et al. 2004) have analyzed the impacts of overexpressing a gene from the CYCD1 subgroup. Of those studies, only Cho et al. (2004) worked with full-sized plants, which permitted the assessment of the phenotype at the plant level. Other studies, although not in the same CYCD subgroup (Riou-Khamlichi et al. 1999; Jasinski et al. 2002; Dewitte et al. 2003), reported curling leaves and small cells in plants overexpressing *AtCYCD3*;*1*, which is similar to what is observed in both our *rippled leaf* and recapitulated plants. De Veylder et al. (2002) also observed a similar leaf alteration phenotype while overexpressing *DPa* (*DRTF* (Database of Rice Transcription Factors) *Polypeptide a*)). This similar phenotype is logical and consistent with an overexpression of *CYCLIN D* as, through association with CDKA, CYCD proteins are known to inactivate RBR by phosphorylation, which ultimately releases the DP-E2F complex to transcribe the multiple genes required for cell cycle progression to take place (Uemukai et al. 2005). This correlates well with the predicted activity of *CYCD1*;*2*, as it is known to be involved in the control of the G1-S transition of the cell cycle that, when overexpressed, should increase cell cycle progression. An increase in cell cycle progression should logically lead to an increase in the absolute number of cells found in the tissue, which is what we see in *rippled leaf*.

The cells in *rippled leaf* are more numerous and smaller; several other studies show that in model species, smaller cortical cells are linked to irregular leaf shape and increased cell division. The overexpression of the *DOWNWARD LEAF CURLING* gene in *Arabidopsis* causes curled leaves, resulting from the reduced size of leaf cells (Kee et al. 2009), and increased expression of *rolA* produces smaller cell size and a wrinkled leaf phenotype in transgenic tobacco (Guivarc'h et al. 1996). The cells may be smaller and organized differently due to either a disruption in cell cycle timing or a decrease in the duration of one or more cell cycle phases. Smaller and more numerous cells may result in an alteration of intracellular spaces, which may in turn alter cellular resource allocation.

Rippled leaf midveins possess a larger vasculature to cortex ratio

In response to the data derived from the longitudinal sections, cross-sections were then analyzed for their proportion of vasculature to cortical tissue. As *rippled leaf* possessed a greater number of cortical cells, it was hypothesized that an analysis of the proportional area would show a greater relative amount of cortex tissue. However, results show that not only does cortical tissue contribute to a smaller proportion of the *rippled leaf* midvein but also the total cross-sectional area of the midvein is less than in WT (Fig. 4). This may also be attributed to heightened cell division. Cell division costs energy; if there is more energy being spent on dividing, less can be spent on growth and overall tissue development. Although there may be more cells, there is a lesser amount of tissue overall because the organism does not have the support systems in place to feed and nurture the increased cell division. The lesser amount of cortical tissue may also be a cause of the abnormal phenotype seen in *rippled leaf*, as the cortex is responsible for protecting and physically supporting the vascular elements.

The phenotype of *rippled leaf* and the transgenic lines overexpressing *PtaCYCD1*;*2* are similar to well-known phenotypes in other woody plants, including corkscrew willow (*Salix matsudana*, Koidz. Cultivar 'Tortuosa') and corkscrew hazel (*Corylus aveellana* L. forma *contorta* (Bean) Rehder) (Klynstra et al. 1964; Lin et al. 2007) (Fig. 6d). These trees have leaves that are rippled and stems that are twisted. Studies with these species have focused more on the stem, given the relationship of the twisted growth with the formation of tension wood. The gene(s) responsible for this trait have not been identified, but the authors suggest that a lack or delay in lignification is responsible for the phenotype (Lin et al. 2007). Additionally, controlled crosses with *C. aveellana* L. forma *contorta* indicate that the twisted trunk and leaf phenotype is controlled by a single recessive gene (Smith and Mechlenbacher 1996). It would be of interest to test whether *CYCD1*;*2* is near the QTL that is associated with the corkscrew willow or whether there is a high level of expression of *CYCD1*;*2* in this tree or if it is related to the single recessive gene in *C. aveellana* L. forma *contorta*.

Rippled leaf altered biomass

Total dry weight biomass was lower in *rippled leaf than* in WT, whereas all characteristics relating to growth—such as plant height and stem diameter at all levels measured—were not significantly higher in *rippled leaf* after 3.5 months' growth. A study done by Gaudin et al. (2000) in snapdragon demonstrated that *CYCD1* transcripts are produced throughout the plant but mainly in the meristems and cells associated throughout the vascular procambial tissues. Increasing cyclin D production in those regions, as observed in other studies, provoked an increase in growth characteristics. Studies supporting this were done by Cho et al. (2004), in which they found increased growth by overexpressing a *CYCD1* in *Arabidopsis*. This increase in plant growth was also demonstrated by Riou-Khamlichi et al. (1999) and Cockcroft et al. (2000) by overexpressing genes from the same family of cyclin D but not from the same subgroup. The Riou-Khamlichi et al. (1999) group demonstrated this by overexpressing *CYCD3*;*1* in *Arabidopsis*, whereas the Cockcroft et al. (2000) group achieved it by overexpressing *CYCD2*;*1*. However, increased plant growth was not observed in *rippled leaf*. Most other studies, in particular the ones that assessed the effects of overexpressing a *CYCD1* homolog, measured cell division activity and growth characteristics (Cho et al. 2004; Koroleva et al. 2004) but not total biomass. Koroleva et al. (2004) measured biomass accumulation, but as their system was cell based using BY-2 cultures, there was no way to assess the impacts of such a change of increased *CYCD1* expression at the whole plant level due to cell expansion and differentiation. Although the impact of overexpression of this gene is most obvious in the leaves, where we can detect the differences in cell number, it seems likely that there is also a less obvious impact on the plant, resulting in the decreased biomass.

Impacts on downstream cell cycle genes

In order to monitor the impacts of an overexpression of *CYCD1*;*2* on known immediate downstream cell cycle genes, the expression of two of its most direct interacting partners, *CDKA* and *RBR*, was assessed. After measuring *CDKA* expression in various tissues, endogenous levels of *CDKA* in WT were found to be highest in stem, petiole, and midvein tissues (Fig. 3e). This is interesting since this pattern is similar to what was found for *CYCD1*;*2* (Fig. 3d). Although patterns are similar, fold difference ratios for *CDKA* barely change in *rippled leaf* when compared with WT which makes sense since the T-DNA enhancer is overexpressing *CYCD1*;*2* and not *CDKA*. This result indicates that there probably is sufficient CDKA available for complex formation with CYCD.

This is supported by the work identifying cyclin D as the rate-limiting factor in the complex for cell cycle transition (Dewitte et al. 2003, 2007; Menges et al. 2006; Qi and John 2007).

In conclusion, a mutant with a leaf alteration phenotype named *rippled leaf* was characterized. The *CYCD1*;*2* gene was found to be responsible for this phenotype. The phenotype was recapitulated using overexpression of transgenic lines. Both the original *rippled leaf* activation-tagged line and the overexpressed lines show the leaf alteration phenotype and increased *CYCD1*;*2* expression as well as an increased number of smaller cells in the cortex. These results suggest that *CYCD1*;*2* gene is responsible for the rippling effect observed. The role of cell cycle in plant development and growth is complex. Further studies with mutants such as *rippled leaf* investigating downstream gene expression of transcriptionally activated genes and evaluating the impact of silencing this gene on the phenotype could enhance our understanding of the basic mechanisms that control cell cycle, in particular in trees. This information is necessary in order to understand many basic questions, such as whether cell division is the driver of growth and development or whether this process simply follows a pre-established developmental plan. Finally, using molecular and microscopy tools to compare these mutant plants with other similar tree phenotypes observed, such as corkscrew willow (*S. matsudana*, Koidz. Cultivar 'Tortuosa') and corkscrew hazel (*C. aveellana* L. forma *contorta* (Bean) Rehder), might lead to a better understanding of the wavy phenotype and altered morphology observed in these trees.

Acknowledgments We would like to thank Laurie Yeates, the manager of the CFS greenhouse, and Terry Hay, Peter Tucker, and Kevin Mann for their advice and care of the mutants. We also thank Ying Chen for technical assistance in creation of the transgenic lines, Dr. Hans-Cees Speel for his willingness to share the photograph of corkscrew willow from bomengids.nl, Dr. Steven Strauss for permission to use a photo taken at his field trial of the activation-tagged lines in Corvallis, Oregon, Liz Clarke for her help in preparing the pictures for the figures and Caroline Simpson for editing the manuscript. This research was funded by the Natural Sciences and Engineering Research Council (SR) and Natural Resources Canada, Canadian Forestry Service A-base funds (TB). The activation-tagged lines were created with Genome Canada funding to SR.

Compliance with ethical standards

Conflict of interest The authors declare that they have no conflict of interest.

Data archiving statement *PtaCYCD1*;*2* cDNA sequence has been submitted to GenBank (accession number KP902591).

References

Arias RS, Filichkin SA, Strauss SH (2006) Divide and conquer: development and cell cycle genes in plant transformation. Trends Biotechnol 24:267–273

Buendía-Monreal M, Rentería-Canett I, Guerrero-Andrade O, Bravo-Alberto CE, Martínez-Castilla LP, García E, Vázquez-Ramos JM (2011) The family of maize D-type cyclins: genomic organization, phylogeny and expression patterns. Physiol Plant 143:297–308

Chang S, Puryear J, Cairney J (1993) A simple and efficient method for isolating RNA from pine trees. Plant Mol Biol Report 11:113–116

Cho JW, Park SC, Shin EA, Kim CK, Han W, Sohn S, Song PS, Wang MH (2004) *Cyclin D1* and $p22^{ack1}$ play opposite roles in plant growth and development. Biochem Biophys Res Commun 324: 52–57

Cockcroft CE, den Boer BGW, Healy JMS, Murray JAH (2000) Cyclin D control of growth rate in plants. Nature 405:575–579

Cui L, Li J, Zhang T, Guo Q, Xu J, Lou Q, Chen J (2014) Identification and expression analysis of D-type cyclin genes in early developing fruit of cucumber (*Cucumis sativus* L.). Plant Mol Biol Report 32: 209–218

De Veylder L, Beeckman T, Beemster GTS, de Almeida EJ, Ormenese S, Maes S, Naudts M, Van Der Schueren E, Jacqmard A, Engler G et al (2002) Control of proliferation, endoreduplication and differentiation by the *Arabidopsis* E2Fa/DPa transcription factor. EMBO J 21: 1360–1368

De Veylder L, Beeckman T, Inzé D (2007) The ins and outs of plant cell cycle. Nat Rev Mol Cell Biol 8:655–665

Dewitte W, Riou-Khamlichi C, Scofield S, Healy JMS, Jacqmard A, Kilby NJ, Murray JAH (2003) Altered cell cycle distribution, hyperplasia, and inhibited differentiation in *Arabidopsis* caused by the D-type cyclin *CYCD3*. Plant Cell 15:79–92

Dewitte W, Scofield S, Alcasabas AA, Maughan SC, Menges M, Braun N, Collins C, Nieuwland J, Prinsen E, Sundaresan V et al (2007) *Arabidopsis CYCD3* D-type cyclins link cell proliferation and endocycles and are rate-limiting for cytokinin responses. Proc Natl Acad Sci 104:14537–14542

Donnelly PM, Bonetta D, Tsukaya H, Dengler RE, Dengler NG (1999) Cell cycling and cell enlargement in developing leaves of *Arabidopsis*. Dev Biol 215:407–419

Erickson RO, Michelini FJ (1957) The plastochron index. Am J Bot 44: 297–304

Gaudin V, Lunness PA, Fobert PR, Towers M, Riou-Khamlichi C, Murray JAH, Coen E, Doonan JH (2000) The expression of D-cyclin genes defines distinct developmental zones in snapdragon apical meristems and is locally regulated by the Cycloidea gene. Plant Physiol 122:1137–1148

Gleave AP (1992) A versatile binary vector system with a T-DNA organisational structure conducive to efficient integration of cloned DNA into the plant genome. Plant Mol Biol 20:1203–1207

Gonzalez N, Vanhaeren H, Inzé D (2012) Leaf size control: complex coordination of cell division and expansion. Trends Plant Sci 17:332–340

Groover A, Robischon M (2006) Developmental mechanisms regulating secondary growth in woody plants. Curr Opin Plant Biol 9:55–58

Guivarc'h A, Carneiro M, Vilaine F, Pautot V, Chriqui D (1996) Tissue-specific expression of the *ROLA* gene mediates morphological changes in transgenic tobacco. Plant Mol Biol 30:125–134

Guo Y, Harwalkar J, Stacey DW, Hitomi M (2005) Destabilization of cyclin D1 message plays a critical role in cell cycle exit upon mitogen withdrawal. Oncogene 24:1032–1042

Gutierrez C (2005) Coupling cell proliferation and development in plants. Nat Cell Biol 7:535–541

Gutierrez C (2009) The Arabidopsis cell division cycle. Arabidopsis Book 7:e0120. doi:10.1199/tab.0120

Harrison EJ, Bush M, Plett JM, McPhee DP, Vitez R, O'Malley B, Sharma V, Bosnich W, Séguin A, MacKay J et al (2007) Diverse developmental mutants revealed in an activation-tagged population of poplar. Can J Bot 85:1071–1081

Hartmann T, Mult S, Suter M, Rennenberg H, Herschbach C (2000) Leaf age-dependent differences in sulphur assimilation and allocation in poplar (*Populus tremula* x *P. alba*) leaves. J Exp Bot 51:1077–1088

Ito M, Iwase M, Kodama H, Lavisse P, Komamine A, Nishihama R, Machida Y, Watanabe A (1998) A novel *cis*-acting element in promoters of plant B-type cyclin genes activates M phase-specific transcription. Plant Cell 10:331–341

Jasinski S, Riou-Khamlichi C, Roche O, Perennes C, Bergounioux C, Glab N (2002) The CDK inhibitor *NtKIS1a* is involved in plant development, endoreduplication and restores normal development of *cyclin D3*;*1*-overexpressing plants. J Cell Sci 115:973–982

Kee JJ, Jun SE, Baek SA, Lee TS, Cho MR, Hwang HS, Lee SC, Kim J, Kim GT, Im KH (2009) Overexpression of the *DOWNWARD LEAF CURLING* (*DLC*) gene from melon changes leaf morphology by controlling cell size and shape in *Arabidopsis* leaves. Mol Cells 28:93–98

Klynstra FB, Lycklama JC, Siebers AM, Burggraaf PD (1964) On the anatomy of the woody stem of the twisted hazel, *Corylus anellana* L. "Contorta". Acta Bot Neerl 13:198–208

Koroleva OA, Tomlinson M, Parinyapong P, Sakvarelidze L, Leader D, Shaw P, Doonan JH (2004) *CYCD1*, a putative G1 Cyclin from *Antirrhinum majus*, accelerates the cell cycle in cultured tobacco BY-2 cells by enhancing both G1/S entry and progression through S and G2 phases. Plant Cell 16:2364–2379

Larson PR, Isebrands JG (1971) The plastochron index as applied to developmental studies of cottonwood. Can J For Res 1:1–11

Lin J, Gunter LE, Harding SA, Kopp RF, McCord RP, Tsai C, Tuskan GA, Smart LB (2007) Development of AFLP and RAPD markers linked to a locus associated with twisted growth in corkscrew willow (*Salix matsudana* "Tortuosa"). Tree Physiol 27:1575–1583

Magyar Z, Mészáros T, Miskolczi P, Deák M, Fehér A, Brown S, Kondorosi E, Athanasiadis A, Pongor S, Bilgin M et al (1997) Cell cycle phase specificity of putative cyclin-dependant kinase variants in synchronized alfalfa cell. Plant Cell 9:223–235

Menges M, Samland AK, Planchais S, Murray JAH (2006) The D-type cyclin *CYCD3*;*1* is limiting for the G1-to-S-phase transition in *Arabidopsis*. Plant Cell 18:893–906

Menges M, Pavesi G, Morandini P, Bögre L, Murray JAH (2007) Genomic organization and evolutionary conservation of plant D-type cyclins. Plant Physiol 145:1558–1576

Oakenfull EA, Riou-Khamlichi C, Murray JAH (2002) Plant D-type cyclins and the control of G1 progression. Philos Trans R Soc Lond B Biol Sci 357:749–760

Perikles S (2003) Q-Gene: processing quantitative real-time RT-PCR data. Bioinformatics 19:1439–1440

Qi R, John PCL (2007) Expression of genomic *AtCYCD2*;*1* in *Arabidopsis* induces cell division at smaller cell sizes: implications for the control of plant growth. Plant Physiol 144:1587–1597

Renaudin JP, Doonan JH, Freeman D, Hashimoto J, Hirt H, Inzé D, Jacobs T, Kouchi H, Rouzé P, Sauter M et al (1996) Plant cyclins: a unified nomenclature for plant A-, B- and D-type cyclins based on sequence organization. Plant Mol Biol 32:1003–1018

Riou-Khamlichi C, Huntley R, Jacqmard A, Murray JAH (1999) Cytokinin activation of *Arabidopsis* cell division through a D-type cyclin. Science 283:1541–1544

Smith DC, Mechlenbacher SA (1996) Inheritance and contorted growth in hazelnut. Euphytica 89:211–213

Smolarkiewicz M, Dhonukshe P (2013) Formative cell divisions: principal determinants of plant morphogenesis. Plant Cell Physiol 54: 333–342

Tsukaya H (2014) Comparative leaf development in angiosperms. Curr Opin Plant Biol 17:103–109

Tuskan GA, Difazio S, Jansson S, Bohlmann J, Grigoriev I, Hellsten U, Putnam N, Ralph S, Rombauts S, Salamov A et al (2006) The genome of black cottonwood, *Populus trichocarpa* (Torr. & Gray). Science 313:1596–1604

Uemukai K, Iwakawa H, Kosugi S, de Uemukai S, Kato K, Kondorosi E, Murray JAH, Ito M, Shinmyo A, Sekine M (2005) Transcriptional activation of tobacco E2F is repressed by co-transfection with the retinoblastoma-related proteins: cyclin D expression overcomes this repressor activity. Plant Mol Biol 57:83–100

Van't Hof J (1966) Experimental control of DNA synthesizing and dividing cells in excised root tips of *Pisum*. Am J Bot 53:970–976

Wang G, Kong H, Sun Y, Zhang X, Zhang W, Altman N, dePamphilis CW, Ma H (2004) Genome-wide analysis of the cyclin family in *Arabidopsis* and comparative phylogenetic analysis of plant cyclin-like proteins. Plant Physiol 135:1084–1099